6926–6934 *Nucleic Acids Research, 2003, Vol. 31, No. 23*
DOI: 10.1093/nar/gkg912

Transient XylR binding to the UAS of the *Pseudomonas putida* σ^{54} promoter *Pu* revealed with high intensity UV footprinting *in vivo*

Marc Valls and Víctor de Lorenzo*

Department of Microbial Biotechnology, Centro Nacional de Biotecnología del Consejo Superior de Investigaciones Científicas (CSIC), Campus de Cantoblanco, 28049 Madrid, Spain

Received August 11, 2003; Revised and Accepted October 16, 2003

ABSTRACT

The binding of the transcriptional regulator XylR to its cognate upstream activating sequences (UAS) of the σ^{54}-dependent promoter *Pu* of *Pseudomonas putida* has been examined *in vivo* in single copy gene dose and stoichiometry. To this end, we have employed a novel *in vivo* genomic footprinting procedure that uses short exposures of bacterial cells to diffuse high intensity UV light that causes formation of TT or TC dimers. In contrast to simpler models for activation of σ^{54}-dependent promoters, our results clearly indicate that the XylR protein is not permanently bound *in vivo* to its target sites in *Pu*. On the contrary, the UAS appear to be mostly unoccupied at all growth stages. This is in contrast to the integration host factor (IHF), which binds *Pu* strongly *in vivo* at stationary phase, as also revealed by UV footprinting. Only overexpression of XylR altered the photoreactivity of the corresponding DNA region to report stable binding of the regulator to the UAS. However, the presence of aromatic XylR inducers reversed the forced occupation caused by increased levels of the activator. These results are compatible with the notion that XylR interacts very transiently with the UAS and detaches from the promoter during transcriptional activation of *Pu*.

INTRODUCTION

The σ^{54}-dependent *Pu* promoter regulates transcription of the *upper* operon of *Pseudomonas putida* mt-2 TOL plasmid pWW0, which encodes the first enzymes for toluene and *m/p*-xylene degradation (1). The RNA polymerase holoenzyme containing σ^{54} (2) can form a closed promoter complex, but is not able to proceed to open complex formation, and thus transcription, in the absence of an activator protein (3–5). XylR is a toluene-responsive activator protein that binds to cognate upstream activating sequences (UAS) of *Pu* (6,7). DNA looping of the region between the UAS and the –12/–24 motifs for the σ^{54}-RNAP seems to facilitate the interaction between the activator protein and the holoenzyme (8–10). In *Pu,* this event is assisted by the integration host factor (IHF), which binds to a specific site in the intervening region (Fig. 1), bringing about a strong DNA bend (11–14). In addition, IHF helps the recruitment of the σ^{54}-RNAP to *Pu* when cells reach stationary phase (15,16).

XylR belongs to the NtrC family of prokaryotic enhancer binding proteins (EBPs), named after the most studied member of the group (17). These regulators exhibit a common mechanism of activation of their cognate promoters. Once exposed to a specific environmental condition (i.e. contact with toluene in the case of XylR), the signal-receiving N-terminal domain of the protein initiates a number of conformational changes leading ultimately to formation of a multimer competent to hydrolyze ATP and drive σ^{54}-dependent transcription initiation (18). With little variation, this seems to be true for virtually all prokaryotic enhancer-binding proteins where the issue has been examined (19–24). Under this view, each of the factors that participate in the activation of a given σ^{54} promoter (EBP, IHF, σ^{54}-RNAP) has an intrinsic ability of interacting with distinct sequences at the corresponding DNA, which in the case of the EBPs may or may not be increased under activation conditions (23,25,26). In either case, the major regulatory step is predicted to be the switching on of the activator already bound to DNA. This simple model is based exclusively on *in vitro* experiments (21–26), where the concentration of every protein can be varied at will. An additional complexity of σ^{54} promoters is the assembly/disassembly of the EBP multimer during transcription. At least in the case of XylR, it seems that the multimeric complex dissociates at every round of transcription. This notion is supported by DNase I footprinting and XylR cross-linking experiments, as well as by the behavior of XylR variants locked in either a multimeric or a non-multimeric state (18). Furthermore, potential intermediates of the cyclic process have been observed *in vitro* by transmission electron microscopy, suggesting that the multimer becomes disassembled every time ATP is hydrolysed (27). Again, all this is based on *in vitro* evidence with a purified and constitutively active form of XylR. But does all this happen *in vivo*?

In this work, we employ a non-disruptive technique (high intensity UV footprinting) for monitoring *in vivo* the occupation of the UAS of *Pu* by XylR under various physiological and induction conditions, but without affecting the single copy

*To whom correspondence should be addressed. Tel: +34 91 585 45 36; Fax: +34 91 585 45 06; Email: vdlorenzo@cnb.uam.es

gene dosage of the regulatory elements and its natural stoichiometry in *P.putida.* The data below indicate that, unlike IHF (which binds *Pu* stably in stationary phase), the interaction of XylR with its cognate UAS in *Pu* is surprisingly transient. Moreover, inducer addition (i.e. XylR activation) further decreases such already weak protein–DNA contacts. These results reinforce the view that the transcriptionally competent complex assembles and disassembles at every initiation round.

MATERIALS AND METHODS

Strains and plasmids

Pseudomonas putida MAD1 is a derivative of the reference *P.putida* strain KT2442 which bears a hybrid mini-Tn*5* transposon encoding the sequence of XylR and a transcriptional *Pu-lacZ* fusion as well (28). This design ensures that all regulatory elements controlling expression from *Pu* are placed in one copy per chromosome. *Pseudomonas putida* MAD2 is identical to *P.putida* MAD1, except that the mini-Tn*5* transposon bears a XylR variant (XylRΔA) which is fully constitutive and requires no inducer for promoter activation. *Pseudomonas putida* SF05 is a strain inserted with the same *Pu-lacZ* fusion as *P.putida* MAD2, but without the *xylR* gene (29). The plasmid used as the template for UV footprinting *in vitro* (pEZ9) has been described before (12). pEZ9 bears an insert spanning coordinates –208 to +93 of the *Pu* sequence. pTK19 plasmid is a derivative of the broad host range plasmid pKT230 harboring a 2.4 kb *Hpa*I fragment from the pWW0 plasmid containing the *xylR* gene expressed under its own promoter (30).

Proteins and enzyme assays

Purified IHF protein of *P.putida* was the kind gift of F. Bartels (GBF, Braunschweig). Purification of the XylRΔA protein fused to a poly-His metallo-affinity tag has been described before (31). As *in vivo* with the *xylRΔA* allele, the XylRΔA protein is a constitutive variant which can fully activate transcription from *Pu* in the absence of any aromatic inducer (31). β-Galactosidase assays were carried out on cells grown in LB medium until the desired optical density (OD_{600}), permeabilized with chloroform and sodium dodecyl sulphate as described by Miller (56). Induced cultures were exposed to saturating vapors of the XylR effector *m*-xylene.

In vitro high intensity UV footprinting

Fifty nanograms of supercoiled pEZ9 plasmid were incubated in a volume of 40 µl for 15 min at 30°C in binding buffer (20 mM Tris–HCl pH 8.0, 2 mM $MgCl_2$, 40 mM KCl, 0.1 mM EDTA, 100 µg/ml bovine serum albumin) in the absence or presence of 400 nM XylRΔA or 100 nM IHF. Following incubation, 20 µl of each mixture were transferred to 0.5 ml Eppendorf tubes, and irradiated for 15–20 s with the UV beam from a 500 W Hg/Xe arc lamp (Oriel Instruments, CT). This instrument produces emissions throughout the UV spectrum, including major peaks at 235, 246, 265, 280, 289, 296, 302 and 315 nm, as well as several emission lines in the infrared (IR) range (820, 880 and 1000 nm). The resulting radiation is thus passed through a water filter (Oriel Instruments, ref. 61955) to eliminate IR. The beam is then collimated in a condenser and carried through a fused silica fiber optics bundle (Oriel Instruments, ref. 77575), the outlet of which is placed at ~15 mm from the treated samples. In this way, the whole UV output of the lamp is concentrated on the DNA–protein sample. After irradiation, the samples were either processed immediately or stored at –20°C. The primer used for extension of the DNA samples was *Pu*14 (5′-CCCGCTTTGAGGA-TATACATGGCGAAAGC-3). *Pu*14 is complementary to positions +63/+91 on the coding strand of the *Pu* promoter. In the presence of *Taq* polymerase and dNTPs, *Pu*14 primes an extension reaction *in vitro* which covers entirely the UAS and the IHF site of *Pu*. This primer was end-labeled with [γ^{32}-P]ATP and T4 polynucleotide kinase (32). For detection of pyrimidine dimers in the DNA, 10 µl of the samples with the irradiated plasmid were added to 6 µl of an amplification mix containing 10 pmol of each of the dNTPs, 1 pmol of the end-labeled primer and 2 U of *Taq* polymerase in 3× GeneAmp PCR buffer with $MgCl_2$ (Perkin Elmer). Samples were then denatured for 3 min at 94°C and subjected to 10 cycles of extension (1 min 94°C, 1 min 61°C, 1 min 72°C) plus a final incubation for 10 min at 72°C. Ten microliters of formamide loading buffer were then added to each sample. Then 2 µl samples were electrophoresed in 6% denaturing polyacrylamide sequencing gels (32). The resulting pattern of radioactive bands was registered in a Molecular Imager System β-sensitive screen and visualized with Quantity One software (Bio-Rad). The different lanes were scanned with the same system and the line graphs were transferred to Microsoft Excel for quantitative analysis. Intensity normalization was performed with respect to the band appearing at position –104, which lies outside both the UASs and the IHF binding site and is therefore unaffected by protein binding.

In vivo UV footprinting

Cultures of *P.putida* MAD1 or *P.putida* MAD2, bearing plasmids or not as indicated, were grown at 30°C in LB liquid medium in the presence or absence of *m*-xylene (see above) until the desired optical densities at 600 (OD_{600}) were reached. Ten 50-µl aliquots of each of the cultures were then dispensed into white Costar™ 96-well plates (Corning Incorporated, Corning, NY) and each well was irradiated for 25–30 s under the same conditions as for the *in vitro* assay above. Replicated samples were immediately collected after treatment, mixed to make 500 µl volumes and chilled at once. The genomic DNA was extracted using the miniprep protocol (32). Ten micrograms of such DNA were used for the primer extension reactions with 5′ labeled oligo Pu*14* described above. These were run in 100 µl volumes, which contained 25 pmol of each dNTP, 5 pmol of labeled primers and 5 U of *Taq* polymerase in a PCR buffer with 2.5 mM $MgCl_2$ as above. Unlike the *in vitro* extensions, the DNA samples from intact cells were submitted to 45 extension cycles (1 min 94°C, 1 min 59°C, 1 min 72°C) and a final extension for 10 min at 72°C. DNA was then precipitated by addition of 10 µl of 3 M sodium acetate, pH 7.5 and 220 µl of ethanol. DNA pellets were rinsed with 70% ethanol, dried and resuspended in 5 µl of TE. After addition of 10 µl of formamide loading buffer (32), 6–7 µl of each reaction were run on a denaturing polyacrylamide gel and analysed as described above. Experiments were repeated at least three times and similar relative band intensities were seen.

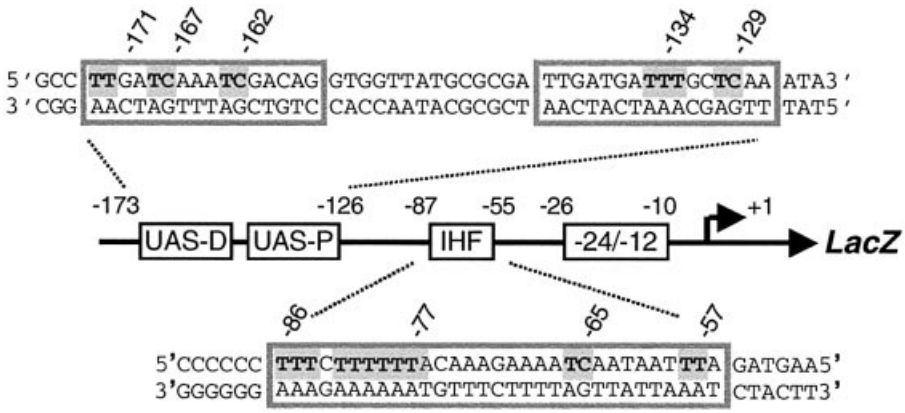

Figure 1. Schematic representation of the *Pu-lacZ* fusion used in this study. The –12/–24 motif for σ^{54}-RNA polymerase recognition, the IHF binding site and the UAS, where the XylR activator binds, are indicated. UAS-D and UAS-P stand, respectively, for the distal and the proximal UAS. The detailed sequence for relevant sites is expanded. Shaded letters indicate adjacent pyrimidine bases that may form dimers upon UV light irradiation. The relative intensity of these bands is a descriptor of specific DNA–protein interactions.

RESULTS AND DISCUSSION

Rationale of UV footprinting for detecting occupation of *Pu* by regulatory proteins

The technique employed in this work for addressing XylR binding to *Pu* under various conditions *in vivo* is based on formation of TT and TC dimers in DNA irradiated with UV light in the range of 230–300 nm (33–36). Since the efficiency of the photochemical reaction is related to the local DNA topology, DNA-binding proteins influence the efficiency of formation of such dimers (37). These changes are revealed by primer extension, since they interfere with DNA polymerization (34). The pattern of such an extension can thus be instrumental for describing the occupation of a given site by a cognate protein. Different variants of this concept have been employed for studying DNA–protein interaction *in vitro* and *in vivo*. For instance, UV-laser footprinting captures the pattern of DNA–protein interactions by subjecting samples to short pulses (~6 ns) of high-energy, coherent 266 nm emissions (38). On the other hand, some features of DNA–protein contacts have been addressed in a few cases by exposing binding mixtures to much longer times (>10 min) of diffuse UV emissions, such as those produced by a commercial transilluminator (39). In our case, we strived to combine the imaging of interactions with a high off rate (as was predicted for XylR-*Pu*, see below) with a relatively short-irradiation period. To this end, we adapted a method in which small sample volumes were irradiated with a non-coherent but high intensity UV light for a few seconds (33), for visualizing *in vivo* XylR binding to the UAS in the chromosome. The technique is operatively referred to as footprinting, although, in reality, what is reflected after UV irradiation is not protection to DNA damage due to bound protein, but the conformation of a DNA segment and its immediate environment.

Prior to examining occupation of *Pu* by XylR, we validated the performance of the UV footprinting procedure. Using UV laser footprinting, we had previously described that binding of IHF to its target site causes a deformation of the DNA helix that is readily converted into increased formation of TT dimers at positions –57 and –81/–77 as well as into hyporeactivity of the –65 CT dimer (16). We compared the pattern of TT/TC bands raised by the binding of IHF *in vitro* to its target site in *Pu* following either a 6 ns UV laser pulse (16) or a 15 s exposure to non-coherent UV beam. The band patterns obtained in the IHF binding site were transformed into intensity plots. The normalized scans of each lane for this region are plotted in Figure 2. Perusal of the results indicates that the intrinsic descriptors of the occupation of the *Pu* promoter by IHF were reproduced at a comparable resolution. We thus assumed that the information revealed by either technique was virtually the same within the scope of this work.

Setting the descriptors of XylR binding to *Pu*

In order to assign the changes in photoreactivity (i.e. band intensity) of *Pu* due to XylR binding, the effect of UV was first examined *in vitro*. Supercoiled pEZ9 plasmid was UV-irradiated in the presence or absence of purified XylRΔA, a constitutively active regulator variant (31). The concentrations of XylRΔA employed in this experiment (400 nM) were those known to produce *in vitro* a detectable DNase I footprint, to form complexes that were visible with electron microscopy and to trigger transcription in an *in vitro* assay (27,31). Following UV exposure, samples were then extended with *Taq* polymerase and products separated in a DNA sequencing gel. The resulting band patterns reporting the physical interaction of XylR with its binding sites are shown in Figure 3. As expected, the changes caused by XylRΔA correspond to termination of primer extension in the vicinity of putative pyrimidine dimers on the template strand (positions –129, –134 in the proximal UAS and –162, –171 in the distal UAS). It is noteworthy that the reactive bases are not identical in each of the UAS, believed to bind XylR dimers separately. This suggests that even unbound DNA has significant local differences in the base–base wedges and their stacking along the DNA helix.

Informative changes in the pattern of pyrimidine dimers did occur upon XylRΔA addition. Inspection of the resulting extension products revealed that the addition of XylRΔA caused a hyper-reactivity of the TC dimer at –162 concurrent with hypo-reactivity of the TT pair at –171 at the distal UAS

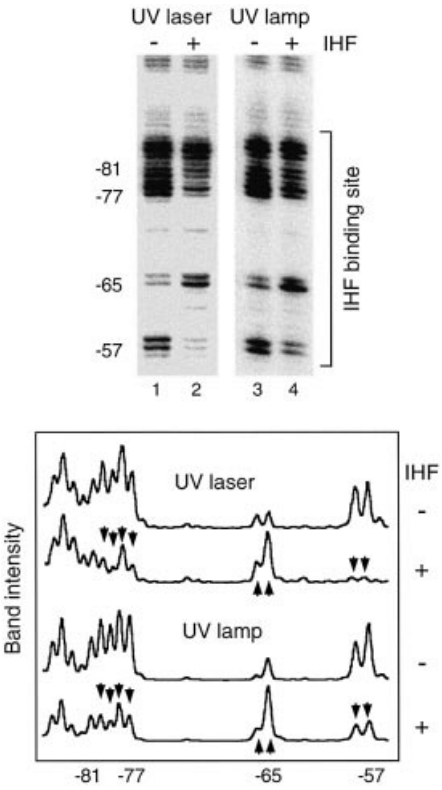

Figure 2. Comparison of UV laser versus non-coherent high intensity UV for DNA footprinting. The gel shows the band patterns obtained after primer extension of the *Pu* promoter irradiated *in vitro* with either a 6 ns UV laser pulse or 15 s of non-coherent UV beam in the presence or absence of the purified IHF protein (see Materials and Methods). The observed photoreactions correspond to formation of dimers between adjacent pyrimidines in the sequence shown in Figure 1. Protein binding alters the physicochemical environment and distorts DNA, affecting such reactivity. This can be visualized after primer extension by changes in band intensities. The gel was scanned and each lane was transformed into a normalized intensity plot shown at the bottom of the figure. It is apparent that formation of pyrimidine dimers occurs in both conditions to a similar extent, and is equally affected by protein binding, resulting in comparable footprints. Compare (lanes 2 and 4) the decreased photoreactivity of positions –77/–81 and –57 and the increase in –65 band intensity upon IHF binding detected by both procedures.

sequence. Similarly, bands at positions –129 and –134 of the proximal UAS region were, respectively, enhanced or weakened upon XylRΔA binding. To obtain a more reliable reference for XylRΔA binding, the bands were scanned, the intensity of the signals normalized with respect to a band that does not appear to vary under any of the conditions tested (–104), and finally plotted as shown in Figure 4. Although changes in the pattern of photoreactivity induced by XylRΔA in *Pu* cannot be interpreted in structural terms, such variations should reflect changes in the wedge angle between bases following XylRΔA binding. Inspection of the scan shown in Figure 4 reveals that bands corresponding to positions –171, –162, –134 and –129, are intrinsic descriptors of the occupation of the *Pu* promoter by XylRΔA, since their relative intensity increases or decreases depending on XylRΔA binding. That XylRΔA caused a sharp reduction in bands –171 and –134, along with a clear augmentation of bands –129 and –162 gave us a useful reference to judge the occupation of the *Pu* promoter *in vivo* as explained below.

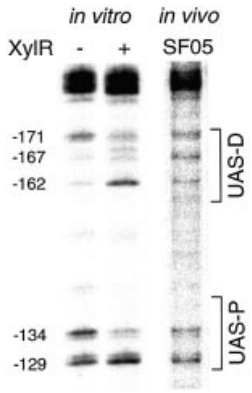

Figure 3. *In vitro* effect of XylR binding to *Pu* and *in vivo* reactivity of the naked promoter. The UV footprinting procedure described in this work was used to monitor the effect of XylR binding on DNA photoreactivity. A supercoiled plasmid bearing *Pu* was UV-irradiated in the presence or absence of the purified XylRΔA protein (a constitutively active variant of the XylR activator). Alternatively, the *Pu-lacZ* but *xylR*-minus strain *P.putida* SF05 was irradiated with UV and its DNA extracted as described in Materials and Methods. In either case, the DNA was extended with a specific primer and the resulting products run in a denaturing polyacrylamide gel. A blow up of the gel zone corresponding to the *Pu* upstream region is shown. Informative positions are indicated on the left. Note the distinct band pattern produced by XylRΔA binding (lane 2), with hyperreactive pyrimidine dimers at –162 and –129 and a hypo-reactivity in –171 and –134. All these positions fall within the well-defined UAS where the XylR regulator binds to bring about transcription activation.

Pu reactivity to UV *in vivo*

Once a reference for XylRΔA binding to *Pu* was produced *in vitro*, we set out to determine whether and under what conditions the regulator was bound to the promoter. Since the target DNA represents a very small fraction of the whole chromosome we adapted the protocol developed for single-copy UV-laser footprint (16) to the new irradiation procedure. With the method described in Materials and Methods, we were able to produce a single-base resolution and signal-to-noise ratio compatible with the results *in vitro.*

To address UAS occupation by XylR *in vivo*, we first subjected cells of *P.putida* SF05 grown in LB to UV irradiation. This strain bears a single-copy insertion of *Pu* but lacks the xylR gene. Therefore, the pattern of pyrimidine dimer formation should reflect the XylR-free state of the DNA region. The result of such a condition is shown in lane 3 of the gel in Figure 3. Comparison of the band pattern *in vivo* versus that *in vitro* allowed an easy match between the major bands found in each case. A positive control is provided by the IHF site, which is occupied by this factor following a well-defined and virtually identical banding arrangement *in vivo* and *in vitro* (see above). As for the UAS, the degree of similarity varies between the proximal and distal sequences. The distinct bands at –134 and –129 were well equivalent *in vitro* and *in vivo* both in intensity and relative ratio. But the status with the distal UAS was different. Although the band at –171 which is predominant *in vitro* appears also *in vivo*, live cells produce an extra band at –167 which is poorly visible *in vitro* (Figs 3 and 4). Furthermore, the extension product at –162, which is produced only weakly *in vitro* in the absence of XylR is clearly apparent *in vivo*.

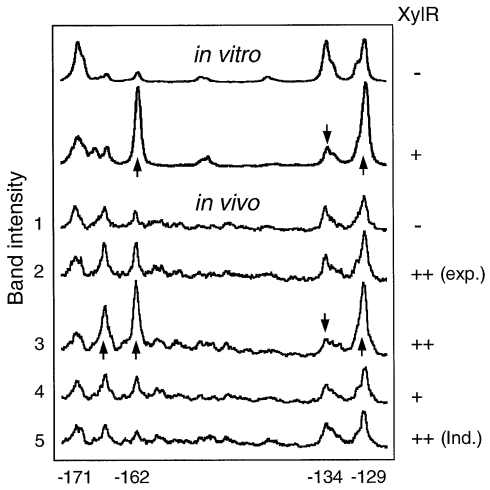

Figure 4. Normalized representation of *in vivo* versus *in vitro* footprints corresponding to the UAS region. The intensity of each signal is represented in arbitrary units. Bands informative of protein binding are identified at the bottom of the scans with respect to the transcription start site. The photoreactivity profiles obtained *in vitro* for the naked DNA (–XylR), and after addition of XylRΔA are shown at the top. An *in vivo* control sample to visualize the reactivity pattern of naked DNA is indicated as Sample 1, and corresponds to *P.putida* SF05 (*Pu-lacZ* but lacking *xylR*) grown to stationary phase. Some discrepancies in the band pattern observed in the non-occupied UAS *in vivo* versus *in vitro* are apparent at the distal UAS (UAS-D), in positions –167 and –162, as discussed in the text. The three scans at the top correspond to the lanes in the gel of Figure 3. The *in vivo* samples 2–5 correspond to those of the experiment in Figure 5, as follows: Sample 2: *P.putida* MAD1 (pTK19) irradiated during exponential growth (exp.), without inducer. Sample 3: *P.putida* MAD1 (pKT19) irradiated at stationary phase, non-induced. Sample 4: Plasmidless *P.putida* MAD1 cells (single copy *Pu-lacZ* and *xylR*), irradiated at stationary phase. Sample 5: *P.putida* MAD1 (pKT19) irradiated at stationary phase after induction with *m*-xylene (ind.). Observe the distinct alteration of band intensity (arrows) upon XylRΔA addition *in vitro*, and the comparable profile obtained *in vivo* only in stationary cells with increased levels of XylR. Note the lack of XylR binding signals in *P.putida* MAD1 (pTK19) cells induced with *m*-xylene.

While the similarity *in vivo* and *in vitro* between the footprints of the proximal UAS with UV is expected, the discrepancies in the distal UAS are not. These differences, which reflect genuine variations in DNA topology *in vivo* and *in vitro*, are the only significant ones throughout the whole promoter region (see below). They are thus unlikely to be caused by variations in local supercoiling or any other reason inherent to DNA alone. Instead, the *in vivo* versus *in vitro* disparity of the UV footprints of distal UAS calls for the presence *in vivo* of an additional factor different from XylR. This factor would bind the sequence and modify the local conformation of DNA, producing the otherwise unlikely CT dimer at –167 and somewhat enhancing the formation of the one at –162. Although we do not know yet the identity of such a putative factor(s), gel retardation assays of radiolabeled UAS with protein extracts of *P.putida* KT2442 indicate the existence of one or more proteins which bind the region in the absence of XylR (Bertoni,G. *et al*., in preparation). Whether or not the two observations are connected (unusual UV footprints in distal UAS in the absence of XylR, factors in *P.putida* other than XylR binding the region) deserves further studies. In any case, the data above reveal the formation *in vivo* of the pyrimidine dimers, which are informative of XylR binding to the UAS. With the cautions triggered by the appearance of an extra band at –167, the evolution of such bands under various growth conditions was then followed and interpreted as explained below.

The UAS of *Pu* stay predominantly clear of bound XylR at any growth stage

We next set out to visualize XylR binding *in vivo* to the *Pu* UAS under conditions ensuring the binding of the factor to target DNA. This is not trivial, since the number of XylR molecules per cell is very low [in the range of 5–30 hexamers/cell (40)] and the resulting intracellular levels are in the 0.5 nM range at its maximum during stationary phase. This figure is several orders of magnitude below the XylRΔA concentrations that produce clear footprints *in vitro*. Furthermore, given the proposed cyclic fashion of *Pu* activation by XylR (18), we expected XylR–UAS interactions to be more stable under non-induced conditions. The reference *in vivo* conditions to examine occupation of UAS by XylR were thus cells of *P.putida* MAD1 (*xylR*$^+$, *Pu-lacZ*) transformed with a multicopy *xylR*$^+$ plasmid (pTK19) in the absence of aromatic inducers. Although, due to its pedigree, pTK19 also bears XylR binding sites (12), this plasmid increases the intracellular concentration of XylR at least 10 times (41) and should thus result in a more favorable occupation of the target sequences. To examine this issue, we grew the *P.putida* MAD1 (pTK19) in LB medium in conditions similar to those used for *P.putida* SF05 above. Samples were collected at the exponential and the stationary phases of growth and irradiated with UV. After the standard processing, reactive pyrimidines were detected as described above. Figure 5 shows the results of this experiment that can be better visualized in the plots of Figure 4. The positive control for the performance of the procedure, and for checking the physiological status of the cell was provided by the IHF site in Pu. As expected, the very specific band pattern indicative of IHF binding did appear in DNA from samples taken at stationary phase (Fig. 5, lanes 2–4), but not in those from exponential growth (Fig. 5, lane 1). As for the UAS region, we detected changes descriptive of XylR binding at both growth stages, in particular the relative ratios of bands –171 versus –162 and –134 versus –129 (Figs 4 and 5). These changes were more visible in samples from stationary cells, perhaps reflecting a further excess in intracellular XylR concentration brought about by the multicopy state of xylR under its own promoter (40). Interestingly, the extra band at –167 in distal UAS was present under all conditions tested and reinforced in the sample from the strain overproducing XylR. This suggested not only that the corresponding DNA distortion involved continues along various growth stages, but also that it is somehow exacerbated by XylR binding.

To examine whether XylR binding to *Pu* could also be detected in *P.putida* cells bearing both *Pu* and xylR in single copy (i.e. in its native stoichiometry), we repeated the procedure with *P.putida* MAD1 strain devoid of any extra plasmid. As shown in Figure 4, the difference between the *P.putida* strains SF05 (*xylR*$^-$) and MAD1 (*xylR*$^+$) through the UAS region was minimal if existing at all, indicating that the corresponding DNA was basically clear of bound XylR. This was in contrast to the distinct attachment of IHF to its downstream target site (Fig. 4). These results are somewhat

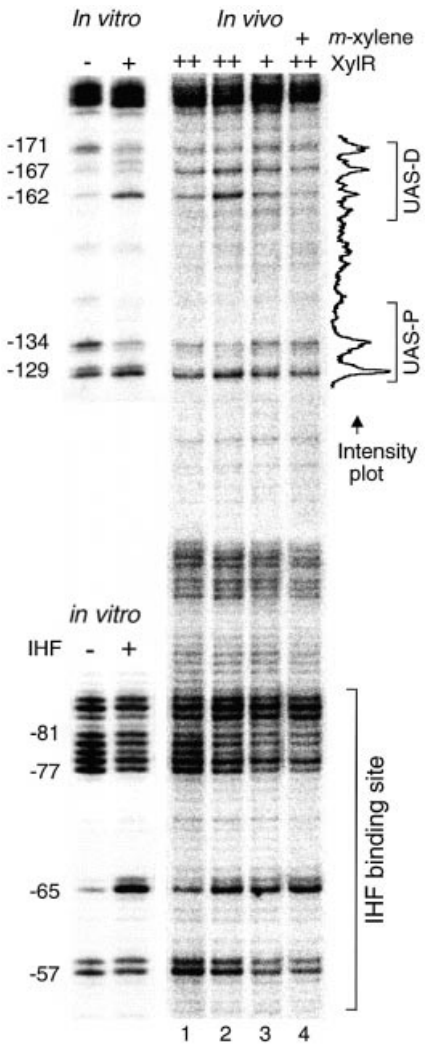

Figure 5. *In vivo* UV footprinting of the *Pu* promoter. Different *P.putida* strains were grown in LB medium as indicated below and exposed to non-coherent UV irradiation. Lane 1: Exponentially growing *P.putida* MAD1 strain (single copy *Pu-lacZ* and *xylR*) transformed with *xylR*$^+$ plasmid pTK19 for increased (++) intracellular levels of XylR protein. Lane 2: *P.putida* MAD1 (pTK19) cells irradiated at stationary phase. Lane 3: stationary *P.putida* MAD1 cells devoid of plasmids and thus containing native intracellular levels (+) of XylR. Lane 4: stationary *P.putida* MAD1 (pTK19) cells induced with *m*-xylene. For reference, *in vitro* footprintings of the UAS and IHF sequences in the absence (–) or presence (+) of the corresponding proteins are shown to the left. Bands informative of protein binding are identified to the left of the gels in respect of the transcription start site. An example of band intensity profile resulting from the scan of lane 4 through the UAS is shown to the right (see full analysis in Fig. 4).

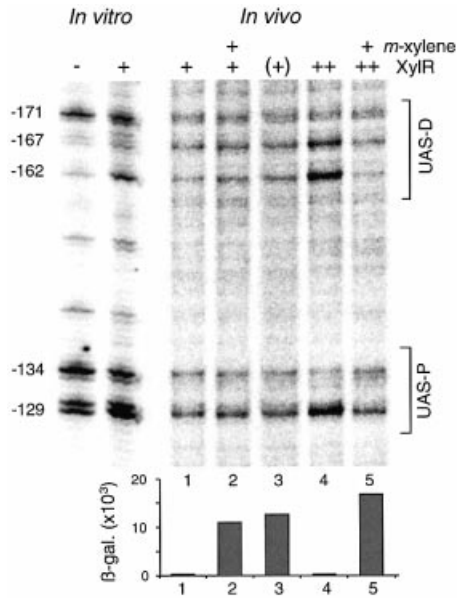

Figure 6. *In vivo* UV footprinting of the UAS of *Pu* promoter in induced versus uninduced *P.putida* cells. For reference, the *in vitro* footprintings of the same region, with indications of relevant nucleotides are shown to the left. All cultures were irradiated at stationary phase. Sample 1: *P.putida* MAD1 non-induced. Sample 2: *P.putida* MAD1, induced with *m*-xylene. Sample 3: *P.putida* MAD2, bearing the constitutive *xylR* allele named *xylRΔA* and thus indicated as (+). Sample 4: *P.putida* MAD1 (pTK19) non-induced. Sample 5: *P.putida* MAD1 (pTK19), induced with *m*-xylene. Note that inducer addition to *P.putida* MAD1 (pTK19) reverses the band changes that describe XylR binding to the UAS (notice bands –167, –162, –134 and –129 in lane 5 versus those of lane 4). The levels of β-galactosidase (Miller units) accumulated by each of the *Pu-lacZ* strains at the moment of irradiation under the conditions specified are represented at the bottom of the gel.

unexpected, as they show that, under non-induced, native conditions the binding of XylR to *Pu* is very poor and altogether insufficient to occupy the UAS permanently. Whether this is due to the low intracellular concentration of the activator, to a poor affinity for the UAS or to competition by already bound factors, only overexpression of XylR gave evidence of binding to *Pu in vivo*.

Transient binding of XylR to *Pu* during promoter activation

That XylR must necessarily bind the UAS *in vivo* for activating transcription was demonstrated because a *Pu* variant deleted of such a region is completely inactive (7,29). On this basis, we inspected the UAS region under conditions where *Pu* is active. This was achieved by either exposing *xylR*$^+$ cells to aromatic inducers such as *m*-xylene or by replacing the wild-type *xylR* gene by its *xylRΔA* counterpart, which encodes the constitutively active XylRΔA protein. Since the bands descriptive of XylR binding *in vitro* and *in vivo* had been identified (see above), we ran a separate experiment to compare the pyrimidine dimer formation patterns of the UAS in cells actively transcribing *Pu*. Such transcriptional activity was followed by virtue of the single copy *Pu-lacZ* fusion built in *P.putida* MAD1 (*xylR*$^+$) and MAD2 (*xylRΔA*$^+$) strains. Lanes 1, 2 and 3 of the gel shown in Figure 6 compare equivalent regions of *P.putida* MAD1 induced or not with *m*-xylene along with the same picture for *P.putida* MAD2. Despite the fact that the *Pu* promoter is being actively transcribed in cells corresponding to samples 2 and 3 (Fig. 6), we could not find any significant difference in the UV footprint of their UAS in respect to those of the inactive *Pu* of sample 1 (at least within the resolution of this technique). This observation rules out the view that inducer addition brings about a real increase in the affinity of XylR for DNA and reinforces the notion that, under native stoichiometry XylR-DNA contacts are as transient as to be elusive to detection with the UV footprinting procedure.

Since occupation of *Pu* under induction could not be revealed *in vivo* with the indigenous concentration of XylR,

we resorted to re-examining the DNA in strain *P.putida* MAD1 (pTK19), which bears higher intracellular levels of XylR (see above). Samples were taken from *m*-xylene-induced and non-induced samples, and the UAS region of each of them processed as usual. The samples were loaded in lanes 4 and 5 of the gel of Figure 6. The most outstanding feature of their comparison was that the increase in the bands which were indicative of *Pu* occupation (–162, –129) reversed their intensity upon exposure to *m*-xylene (a higher resolution picture of the same effect can be seen in lane 4 of the gel of Fig. 5). This suggested that during *Pu* functioning, the already weak binding of XylR to the promoter is destabilized rather than increased. In any case, these observations revealed a new view of the functioning of *Pu in vivo* that diverges from the simpler view of most σ^{54} promoters, in which the EBP is mostly bound to the UAS irrespective of the level of transcription (5). In the well-studied case of NtrC (42), there is evidence for stable binding of this archetypical EBP to the *glnAp1* and *glnL* promoters under physiological conditions. Yet, this may not be a general feature of every σ^{54} promoter: our observations open the possibility that such EBP-DNA binding can itself be regulated by additional factors and environmental conditions.

CONCLUSION

We have shown previously that the intracellular concentration of both IHF (16) and XylR (40) in *P.putida* varies during growth. In the case of IHF, we demonstrated that the levels of the factor during exponential growth are insufficient to saturate the *Pu* promoter (16). This is seen not only in the loss of optimal promoter geometry (13,43), but also in the lack of recruitment of σ^{54}-RNAP to the promoter (15). As a consequence, the transcriptional capacity of *Pu* is very low during exponential growth but extraordinarily high in the stationary phase. In addition to IHF, the level of XylR itself is subject to some degree of growth-phase control, as the number of XylR molecules (monomers) increases from 30 to 120. If [as believed for other EBPs (24,44,45)], the active form of XylR is a hexamer or a larger oligomer, then the number of active XylR species is extremely limited and changes in concentration with growth could have a regulatory effect. As described above, we set out to examine *Pu* occupation by XylR under various conditions adapting the least disruptive *in vivo* footprinting procedure available, based on short-time UV irradiation of cell cultures.

The most salient conclusion of the experiments above is the lack of stable binding of XylR to its target sites at the *Pu* promoter. Only when XylR was overexpressed could the pyrimidine dimer formation pattern through the UAS *in vivo* be matched with that raised by the purified XylRΔA protein on *Pu* DNA *in vitro*. We believe that this result is not due to a lack of sensitivity of the technique employed, but it reflects the bona fide state of the promoter under physiological conditions. More intricate explanations (e.g. formation of a different type of protein–DNA complex which may not be detected with UV footprinting) cannot be ruled out. But on the basis of the data available we must favor the simpler view. Parallel experiments run with much shorter pulses of high-energy UV-laser on the same samples gave basically the same results (not shown). The lack of occupation of *Pu* by XylR contrasts with the evident interaction of IHF with its target in cells at stationary phase, as revealed both with UV-laser footprinting (16,46) and high intensity UV irradiation (this work). The results described in this work add to the notion that proteins present in small number in the cell may exhibit a distinct behavior, in which the DNA–protein interactions are hardly explained by classical thermodynamic equations (47). The low concentration of XylR in the cell, and its weak interactions with the UAS make it plausible that XylR multimerization—an event that is crucial for *Pu* activation (18)—could occur in solution before contacting *Pu*. It could even happen that the activator multimer interacts with σ^{54} or the RNA holoenzyme prior to DNA binding. Such a pre-recruitment type of mechanism has recently been described for the SoxR regulator in *E.coli* (48) and could also be present in other cases.

It is revealing to compare our results with those reported in 1991 by Abril *et al*. using dimethyl sulphate as the footprinting agent *in vivo* (11). In this case, the authors employed *E.coli* as the host to probe XylR–*Pu* interactions in a multicopy set-up in which the *xylR* gene was present in large excess. Changes in the UAS region were detected in the presence or absence of XylR, as well as in induced versus non-induced conditions. Yet, such an assay system did not maintain either the native host of the system or the stoichiometry of the regulatory elements, so it failed to detect the clearance of *Pu* under most circumstances. In our hands, only the artificial overproduction of XylR allowed visualization of protein binding to *Pu in vivo*, as compared to the singular conditions pondered by Abril *et al*. (11).

Despite these limitations, we could still picture the effect of inducer addition in the binding of XylR to *Pu* by forcing a longer term occupation of the promoter by an increased intracellular concentration of the regulator (Figs 4 and 6). The unanticipated result of these experiments was that inducer addition (and the predicted activation or XylR to a transcription-competent form) decreased, rather than increased the binding of XylR to its target DNA. This may be due to the fact that intracellular concentrations of XylR appear to decrease upon inducer addition, conceivably due to a higher protein turnover (40). In addition, the binding can be further reduced by the disassembly of the upstream nucleoprotein complex at every transcription round, as has been proposed not only for *Pu* (18,27) but also for the *glnAp2* promoter of *E.coli* (49). In any case, it does appear that XylR is not strongly bound to *Pu* under any circumstance thereby allowing extra regulatory checks that increase or further decrease such an interaction. In this respect, the possibility of an extra factor binding the distal UAS (as hinted at by the TC dimer at –167 *in vivo*, see above) deserves future studies.

The main paradox between the functioning of σ^{54} promoters *in vivo* and *in vitro* is that factor binding to the corresponding DNA sequence is not granted in live bacteria. In fact, that the whole initiation complex is re-assembled at every transcription round might be a general trait of σ^{54} promoters (49). In our case, there is only an invariable number of ~80 U of σ^{54} per *P.putida* cell (40), which may appear insufficient for saturation of the ~50 σ^{54}-promoters in the genome (50) and for efficient sigma factor competition for available core RNA polymerase (51). Only at stationary stage does IHF reach intracellular levels high enough to saturate *Pu*, and perhaps many other IHF-dependent σ^{54}-promoters. The amount of

XylR (and perhaps other EBPs as well) also varies in a growth-dependent fashion and is only transiently bound to the UAS. It is possible that each of these variables are connected to specific physiological conditions, so that promoter output can be finely tuned to the degree of transcription required in the diversity of environments where *P.putida* thrives (52,53). In this respect, we advocate that the organization and functioning of σ^{54}-promoters is particularly well suited for interweaving a large number of physiological signals in the final transcriptional output (53–55).

NOTE ADDED IN PROOF

Lee *et al*. (57) have recently reported that the active form of an enhancer-binding protein is a heptamer.

ACKNOWLEDGEMENTS

The authors are indebted to V. Shingler and T. Galvao for critical reading of the manuscript and to F. Velázquez and M. Mencía for inspiring discussions. This work was supported in part by contracts QLK3-CT-2002-01933, QLK3-CT-2002-01923, and INCO-CT-2002-1001, by grant BIO2001-2274 of the Spanish Comisión Interministerial de Ciencia y Tecnología (CICYT) and by the Strategic Research Groups Program of the Autonomous Community of Madrid. M.V. is a beneficiary of the I3P Programme of the CSIC.

REFERENCES

1. Ramos,J.L. and Marqués,S. (1997) Transcriptional control of the *Pseudomonas* TOL plasmid catabolic operons is achieved through an interplay of host factors and plasmid-encoded regulators. *Annu. Rev. Microbiol.*, **51**, 341–373.
2. Merrick,M. (1993) In a class of its own—the RNA polymerase sigma factor σ^{54} (σ^{N}). *Mol. Microbiol.*, **10**, 903–909.
3. Buck,M., Gallegos,M.T., Studholme,D.J., Guo,Y. and Gralla,J.D. (2000) The bacterial enhancer-dependent σ^{54} (σ^{N}) transcription factor. *J. Bacteriol.*, **182**, 4129–4136.
4. Popham,D.L., Szeto,D., Keener,J. and Kustu,S. (1989) Function of a bacterial activator protein that binds to transcriptional enhancers. *Science*, **243**, 629–635.
5. Sasse-Dwight,S. and Gralla,J.D. (1988) Probing the *Escherichia coli glnALG* upstream activation mechanism *in vivo*. *Proc. Natl Acad. Sci. USA*, **85**, 8934–8938.
6. Abril,M.A. and Ramos,J.L. (1993) Physical organization of the upper pathway operon promoter of the *Pseudomonas* TOL plasmid. Sequence and positional requirements for XylR-dependent activation of transcription. *Mol. Gen. Genet.*, **239**, 281–288.
7. Pérez-Martín,J. and de Lorenzo,V. (1996) Physical and functional analysis of the prokaryotic enhancer of the σ^{54}-promoters of the TOL plasmid of *Pseudomonas putida*. *J. Mol. Biol.*, **258**, 562–574.
8. Wedel,A., Weiss,D.S., Popham,D., Dröge,P. and Kustu,S. (1990) A bacterial enhancer functions to tether a transcriptional activator near a promoter. *Science*, **248**, 486–490.
9. Carmona,M., Claverie-Martín,F. and Magasanik,B. (1997) DNA bending and the initiation of transcription at σ^{54}-dependent bacterial promoters. *Proc. Natl Acad. Sci. USA*, **94**, 9568–9572.
10. Xu,H. and Hoover,T.R. (2001) Transcriptional regulation at a distance in bacteria. *Curr. Opin. Microbiol.*, **4**, 138–144.
11. Abril,M.A., Buck,M. and Ramos,J.L. (1991) Activation of the *Pseudomonas* TOL plasmid upper pathway operon. *J. Biol. Chem.*, **266**, 15832–15838.
12. deLorenzo,V., Herrero,M., Metzke,M. and Timmis,K.N. (1991) An upstream XylR- and IHF-induced nucleoprotein complex regulates the sigma 54-dependent *Pu* promoter of TOL plasmid. *EMBO J.*, **10**, 1159–1167.
13. Pérez-Martín,J., Timmis,K.N. and de Lorenzo,V. (1994) Co-regulation by bent DNA. Functional substitutions of the integration host factor site at σ^{54}-dependent promoter *Pu* of the upper-TOL operon by intrinsically curved sequences. *J. Biol. Chem.*, **269**, 22657–22662.
14. Seong,G.H., Kobatake,E., Miura,K., Nakazawa,A. and Aizawa,M. (2002) Direct atomic force microscopy visualization of integration host factor-induced DNA bending structure of the promoter regulatory region on the *Pseudomonas* TOL plasmid. *Biochem. Biophys. Res. Commun.*, **291**, 361–366.
15. Bertoni,G., Fujita,N., Ishihama,A. and de Lorenzo,V. (1998) Active recruitment of sigma54-RNA polymerase to the *Pu* promoter of *Pseudomonas putida*: role of IHF and αCTD. *EMBO J.*, **17**, 5120–5128.
16. Valls,M., Buckle,M. and de Lorenzo,V. (2002) *In vivo* UV laser footprinting of the *Pseudomonas putida* sigma 54 *Pu* promoter reveals that integration host factor couples transcriptional activity to growth phase. *J. Biol. Chem.*, **277**, 2169–2175.
17. Morett,E. and Segovia,L. (1993) The σ^{54} bacterial enhancer-binding protein family: mechanism of action and phylogenetic relationship of their functional domains. *J. Bacteriol.*, **175**, 6067–6074.
18. Perez-Martin,J. and de Lorenzo,V. (1996) ATP binding to the sigma 54-dependent activator XylR triggers a protein multimerization cycle catalyzed by UAS DNA. *Cell*, **86**, 331–339.
19. Hwang,I., Thorgeirsson,T., Lee,J., Kustu,S. and Shin,Y.K. (1999) Physical evidence for a phosphorylation-dependent conformational change in the enhancer-binding protein NtrC. *Proc. Natl Acad. Sci. USA*, **96**, 4880–4885.
20. Wang,Y.K., Lee,J.H., Brewer,J.M. and Hoover,T.R. (1997) A conserved region in the σ^{54}-dependent activator DctD is involved in both binding to RNA polymerase and coupling ATP hydrolysis to activation. *Mol. Microbiol.*, **26**, 373–386.
21. Lee,H.S., Berger,D.K. and Kustu,S. (1993) Activity of purified NIFA, a transcriptional activator of nitrogen fixation genes. *Proc. Natl Acad. Sci. USA*, **90**, 2266–2270.
22. Bordes,P., Wigneshweraraj,S.R., Schumacher,J., Zhang,X., Chaney,M. and Buck,M. (2003) The ATP hydrolyzing transcription activator phage shock protein F of *Escherichia coli*: Identifying a surface that binds sigma 54. *Proc. Natl Acad. Sci. USA*, **100**, 2278–2283.
23. Tropel,D. and van der Meer,J.R. (2002) Identification and physical characterization of the HbpR binding sites of the *hbpC* and *hbpD* promoters. *J. Bacteriol.*, **184**, 2914–2924.
24. Wikstrom,P., O'Neill,E., Ng,L.C. and Shingler,V. (2001) The regulatory N-terminal region of the aromatic-responsive transcriptional activator DmpR constrains nucleotide-triggered multimerisation. *J. Mol. Biol.*, **314**, 971–984.
25. Wang,X.Y., Kolb,A., Cannon,W. and Buck,M. (1997) Nucleoprotein complex formation by the enhancer binding protein NifA. *Nucleic Acids Res.*, **25**, 3478–3485.
26. Wyman,C., Rombel,I., North,A.K., Bustamante,C. and Kustu,S. (1997) Unusual oligomerization required for activity of NtrC, a bacterial enhancer-binding protein. *Science*, **275**, 1658–1661.
27. Garmendia,J. and de Lorenzo,V. (2000) Visualization of DNA–protein intermediates during activation of the *Pu* promoter of the TOL plasmid of *Pseudomonas putida*. *Microbiology*, **146**, 2555–2563.
28. Fernandez,S., de Lorenzo,V. and Perez-Martin,J. (1995) Activation of the transcriptional regulator XylR of *Pseudomonas putida* by release of repression between functional domains. *Mol. Microbiol.*, **16**, 205–213.
29. Fernandez,S., Shingler,V. and De Lorenzo,V. (1994) Cross-regulation by XylR and DmpR activators of *Pseudomonas putida* suggests that transcriptional control of biodegradative operons evolves independently of catabolic genes. *J. Bacteriol.*, **176**, 5052–5058.
30. deLorenzo,V., Fernandez,S., Herrero,M., Jakubzik,U. and Timmis,K.N. (1993) Engineering of alkyl- and haloaromatic-responsive gene expression with mini-transposons containing regulated promoters of biodegradative pathways of *Pseudomonas*. *Gene*, **130**, 41–46.
31. Pérez-Martín,J. and de Lorenzo,V. (1996) *In vitro* activities of an N-terminal truncated form of XylR, a σ^{54}-dependent transcriptional activator of *Pseudomonas putida*. *J. Mol. Biol.*, **258**, 575–587.
32. Ausubel,F.M., Brent,R., Kingston,R.E., Moore,D.D., Seidman,J.G., Smith,J.A. and Struhl,K. (1994) *Current Protocols in Molecular Biology*. John Wiley and Sons, New York.
33. Becker,M.M. and Wang,J.C. (1984) Use of light for footprinting DNA *in vivo*. *Nature*, **309**, 682–687.

34. Buckle,M., Geiselmann,J., Kolb,A. and Buc,H. (1991) Protein–DNA cross-linking at the *lac* promoter. *Nucleic Acids Res.*, **19**, 833–840.
35. Kuluncsics,Z., Perdiz,D., Brulay,E., Muel,B. and Sage,E. (1999) Wavelength dependence of ultraviolet-induced DNA damage distribution: involvement of direct or indirect mechanisms and possible artefacts. *J. Photochem. Photobiol. B Biol.*, **49**, 71–80.
36. Gurzadyan,G.G., Gorner,H. and Schulte-Frohlinde,D. (1995) Ultraviolet (193, 216 and 254 nm) photoinactivation of *Escherichia coli* strains with different repair deficiencies. *Radiat. Res.*, **141**, 244–251.
37. Engelhorn,M., Boccard,F., Murtin,C., Prentki,P. and Geiselmann,J. (1995) *In vivo* interaction of the *Escherichia coli* integration host factor with its specific binding sites. *Nucleic Acids Res.*, **23**, 2959–2965.
38. Hockensmith,J.W., Kubasek,W.L., Vorachek,W.R. and von Hippel,P.H. (1993) Laser cross-linking of proteins to nucleic acids. I. Examining physical parameters of protein-nucleic acid complexes. *J. Biol. Chem.*, **268**, 15712–15720.
39. Buck,M. and Cannon,W. (1994) A simple procedure for visualising protein-nucleic acid complexes by photochemical crosslinking. *Nucleic Acids Res.*, **22**, 1119–1120.
40. Fraile,S., Roncal,F., Fernandez,L.A. and de Lorenzo,V. (2001) Monitoring intracellular levels of XylR in *Pseudomonas putida* with a single-chain antibody specific for aromatic-responsive enhancer-binding proteins. *J. Bacteriol.*, **183**, 5571–5579.
41. Garmendia,J. and de Lorenzo,V. (2000) The role of the interdomain B linker in the activation of the XylR protein of *Pseudomonas putida*. *Mol. Microbiol.*, **38**, 401–410.
42. Shiau,S.P., Schneider,B.L., Gu,W. and Reitzer,L.J. (1992) Role of nitrogen regulator I (NtrC), the transcriptional activator of *glnA* in enteric bacteria, in reducing expression of glnA during nitrogen-limited growth. *J. Bacteriol.*, **174**, 179–185.
43. Pérez-Martín,J. and de Lorenzo,V. (1995) Integration host factor suppresses promiscuous activation of the σ^{54}-dependent promoter *Pu* of *Pseudomonas putida*. *Proc. Natl Acad. Sci. USA*, **92**, 7278–7281.
44. Farez-Vidal,M.E., Wilson,T.J., Davidson,B.E., Howlett,G.J., Austin,S. and Dixon,R.A. (1996) Effector-induced self-association and conformational changes in the enhancer-binding protein NtrC. *Mol. Microbiol.*, **22**, 779–788.
45. Rippe,K., Guthold,M., Hippel,P.H. and Bustamante,C. (1997) Transcriptional activation via DNA-looping: visualization of intermediates in the activation pathway of *E.coli* RNA polymerase σ^{54} holoenzyme by scanning force microscopy. *J. Mol. Biol.*, **270**, 125–138.
46. Murtin,C., Engelhorn,M., Geiselmann,J. and Boccard,F. (1998) A quantitative UV laser footprinting analysis of the interaction of IHF with specific binding sites: re-evaluation of the effective concentration of IHF in the cell. *J. Mol. Biol.*, **284**, 949–961.
47. Halling,P.J. (1989) Do the laws of chemistry apply to living cells? *Trends Biochem. Sci.*, **14**, 317–318.
48. Griffith,K.L., Shah,I.M., Myers,T.E., O'Neill,M.C. and Wolf,R.E. (2002) Evidence for 'pre-recruitment' as a new mechanism of transcription activation in *Escherichia coli*: the large excess of SoxS binding sites per cell relative to the number of SoxS molecules per cell. *Biochem. Biophys. Res. Commun.*, **291**, 979–986.
49. Bondarenko,V., Liu,Y., Ninfa,A. and Studitsky,V.M. (2002) Function of prokaryotic enhancer over a distance does not require continued presence of promoter-bound sigma54 subunit. *Nucleic Acids Res.*, **30**, 636–642.
50. Cases,I. and de Lorenzo,V. (2003) The sigma 54 regulon (sigmulon) of *Pseudomonas putida*. *Microbiology*, in press.
51. Laurie,A.D., Bernardo,L.M., Sze,C.C., Skarfstad,E., Szalewska-Palasz,A., Nystrom,T. and Shingler,V. (2003) The role of the alarmone (p)ppGpp in sigma N competition for core RNA polymerase. *J. Biol. Chem.*, **278**, 1494–1503.
52. Cases,I. and de Lorenzo,V. (2001) The limits to genomic predictions: role of σ^{N} in environmental stress survival of *Pseudomonas putida*. *FEMS Microbiol. Ecol.*, **35**, 217–221.
53. Shingler,V. (2003) Integrated regulation in response to aromatic compounds: from signal sensing to attractive behaviour. *Environ. Microbiol.*, in press.
54. Cases,I. and de Lorenzo,V. (2001) The black cat/white cat principle of signal integration in bacterial promoters. *EMBO J.*, **20**, 1–11.
55. Cases,I., Lopez,J.A., Albar,J.P. and de Lorenzo,V. (2001) Evidence of multiple regulatory functions for the PtsN (IIA(Ntr)) protein of *Pseudomonas putida*. *J. Bacteriol.*, **183**, 1032–1037.
56. Miller,J.H. (1972) *Experiments in Molecular Genetics*. Cold Spring Harbor Laboratory Press, Cold Spring Harbor, NY.
57. Lee,S.Y., De La Torre,A., Yan,D., Kustu,S., Nixon,B.T. and Wemmer,D.E. (2003) Regulation of the transcriptional activator NtrC1: structural studies of the regulatory and AAA+ ATPase domains. *Genes Dev.*, **17**, 2552–2563.